Impact of the Urban Heat Island Effect on Precipitation over a Complex Geographic Environment in Northern Taiwan

CHUAN-YAO LIN AND WAN-CHIN CHEN

Research Center for Environmental Changes, Academia Sinica, Taipei, Taiwan

PAO-LIANG CHANG

Central Weather Bureau, Taipei, Taiwan

YANG-FAN SHENG

Research Center for Environmental Changes, Academia Sinica, Taipei, Taiwan

(Manuscript received 4 March 2010, in final form 29 September 2010)

ABSTRACT

To evaluate the impacts of the urban heat island (UHI) effect on precipitation over a complex geographic environment in northern Taiwan, the next-generation mesoscale model, the Weather Research and Forecasting (WRF) model, coupled with the Noah land surface model and urban canopy model (UCM), was used to study this issue. Based on a better land use classification derived from Moderate Resolution Imaging Spectroradiometer (MODIS) satellite data (the MODIS case), it has significantly improved simulation results for the accumulation rainfall pattern as compared with the original U.S. Geological Survey (USGS) 25-category land use classification (the USGS case). The precipitation system was found to develop later but stronger in the urban (MODIS) case than in the nonurban (USGS) case. In comparison with the observation by radar, simulation results predicted reasonably well; not only was the rainfall system enhanced downwind of the city over the mountainous area, but it also occurred at the upwind plain area in the MODIS case. The simulation results suggested that the correct land use classification is crucial for urban heat island modeling study. The UHI effect plays an important role in perturbing thermal and dynamic processes; it affects the location of thunderstorms and precipitation over the complex geographic environment in northern Taiwan.

1. Introduction

The significance of the interactions between urbanization and the atmosphere environment is becoming more and more evident. Rapid progress in industrialization and urbanization has resulted in environmental problems such as increasing energy consumption and air pollution, deterioration of visibility, a significant urban heat island (UHI) effect, and even local (regional) climate change. (Oke 1982; Grimmond and Oke 1995; Atkinson 2003; Arnfield 2003; Jin et al. 2005; Feddema et al. 2005; Ren et al. 2007; Corburn 2009).

The UHI effect is due to land use changes, which result in changing physical properties such as albedo, surface roughness, evapotranspiration and energy flux, and in turn change climate systems. Several researchers have noted that the UHI effect has a significant impact on mesoscale circulation and that it results in convection and precipitation (e.g., Bornstein 1968; Oke 1982; Balling and Cerveny 1987; Lo et al. 1997; Bornstein and Lin 2000; Morris et al. 2001; Shepherd 2005; Dixon and Mote 2003; Pielke et al. 2007; Lin et al. 2008a,b).

The impact of the UHI effect on rainfall could be either enhancement (Naccarato et al. 2003; Dixon and Mote 2003; Shepherd et al. 2002; Mote et al. 2007) or initiation (Rozoff et al. 2003; Bornstein and Lin 2000; Baik et al. 2001) thereof, depending on the size of the city and its surrounding geographic features. Shepherd et al. (2002) suggested that within 30–60 km downwind of the metropolis, the average increase in monthly rainfall could be as high as 28%. This is due to the preferential heating of the city as compared with the surrounding area, which results in increased instability and convective activities over

Corresponding author address: Chuan Yao Lin, Research Center for Environmental Changes, Academia Sinica, No. 128, Sec. 2, Academia Rd., Taipei 115, Taiwan.
E-mail: yao435@rcec.sinica.edu.tw

DOI: 10.1175/2010JAMC2504.1

downwind areas of the city. The investigations of Steiger et al. (2002) over Atlanta, Georgia, as well as earlier studies in other cities have convincingly demonstrated this effect. Furthermore, theoretical and numerical studies (Hjemfelt 1982; Thielen et al. 2000; Baik et al. 2001; Rozoff et al. 2003; Lin et al. 2008a; Shem and Shepherd 2009) have suggested that urbanization increases surface roughness and could enhance surface convergence. Other than the dynamical and thermal effects of urbanization, increased condensation by aerosols over the city also plays a vital role in precipitation (Baik et al. 2001; Shepherd 2005; van den Heever and Cotton 2007; Lacke et al. 2009).

For the modeling study, detailed land use and urban parameters are critical to simulate the UHI impact. Kusaka and Kimura (2004) implemented urban canopy parameterization in a mesoscale model to improve the modeling performance in their urban boundary layer study. Chen and Dudhia (2001) indicated that the land surface model (LSM) has played a very important role in studying the development of the boundary layer and land–sea circulation. Recently, the Weather Research and Forecasting (WRF) model has been coupled with the Noah land surface and urban canopy model (UCM) (Tewari et al. 2006; Holt and Pullen 2007; Lin et al. 2008b). Lin et al. (2008b) applied this combined WRF-Noah-UCM model to study the UHI issue over northern Taiwan. From the model simulation results under the correct land use classification they found that anthropogenic heat plays an important role in boundary layer development and land–sea circulation due to thermal forcing increase.

Taiwan, especially Taipei (the largest city, located in northern Taiwan; Fig. 1), is experiencing a significant UHI effect due to its location in a basin surrounded by high mountains. It has a very high population density; more than six million people, about one-quarter of the total population of Taiwan, inhabit this basin. Such a high population density and complex geographic structure makes the effect of UHI in Taipei significantly more severe than in other cities of similar scale around the world. For example, Chen et al. (2007) indicated that the daily mean temperature in Taipei shows an increase of 1.5°C due to urbanization. Lin et al. (2008b) found that the UHI intensity in Taipei could be as high as 4°–6°C.

The UHI effect over the Taipei basin should also have a significant impact on precipitation (Chen et al. 2007). However, to date, the fundamental understanding of the impact of UHI on precipitation over the Taipei metropolis has not been well documented. As we know, mountains significantly influence thermal and dynamical effects as well as the formation of precipitation systems (Lin and Chen 2002; C. Chen et al. 2004, 2005). It is expected that the impact of UHI effect over this unique geographic location is significantly different from other cities located on a large plain. Thus, the role of the UHI effect in such a complex geographic location and its impact on precipitation are the major considerations of this study.

In this study, radar, surface meteorological stations, and radio soundings provided by the Central Weather Bureau (CWB) have been used to analyze the study case. According to our previous experience (Lin et al. 2008b), the WRF-Noah-UCM model has significantly improved boundary prediction because of its inclusion of detailed parameters of sensible and latent heat flux, soil heat flux, and anthropogenic materials. Therefore, we have further applied this model to evaluate the impact of the UHI effect on the development of rainfall systems over the complex geography of northern Taiwan.

2. WRF-Noah urban canopy modeling system and land use distribution

a. WRF-Noah urban canopy modeling system

The WRF model is a next-generation mesoscale meteorological model; it is described in detail by Skamarock et al. (2005). To improve the UHI influence and to correctly estimate energy consumption in urban areas, an advanced Noah (Ek et al. 2003) land surface–hydrology model has been coupled to the WRF model (F. Chen et al. 2004; Tewari et al. 2006). The Noah-LSM model provides surface sensible and latent heat fluxes and surface skin temperature in the lower boundary (Chen and Dudhia 2001; Ek et al. 2003). This LSM model is based on the coupling of the diurnally dependent Penman potential evaporation approach, the multilayer soil model, and the primitive canopy model (Chen and Dudhia 2001). The Noah–LSM model has a single vegetation canopy layer and the following prognostic variables: soil moisture and temperature in the soil layer, water stored in the canopy, and snow stored on the ground (F. Chen et al. 2004). Furthermore, in order to better represent the physical processes involved in the exchange of heat, momentum, and water vapor in the mesoscale model, an urban canopy model has been coupled to the WRF model (Kusaka et al. 2006; Tewari et al. 2006).

The UCM is a single-layer model used to consider the effects of urban geometry on surface energy balance and wind shear for urban regions (Kusaka et al. 2001; Kusaka and Kimura 2004). This model includes shadows from buildings, canyon orientation, diurnal variation of azimuth angle, reflection of shortwave and longwave radiation, wind profiles in the canopy layer, anthropogenic heating associated with energy consumption by human activities, and multilayer heat transfer equation for roof, wall, and road surfaces. [For a detailed description of this urban canopy model, see Kusaka and Kimura (2004)].

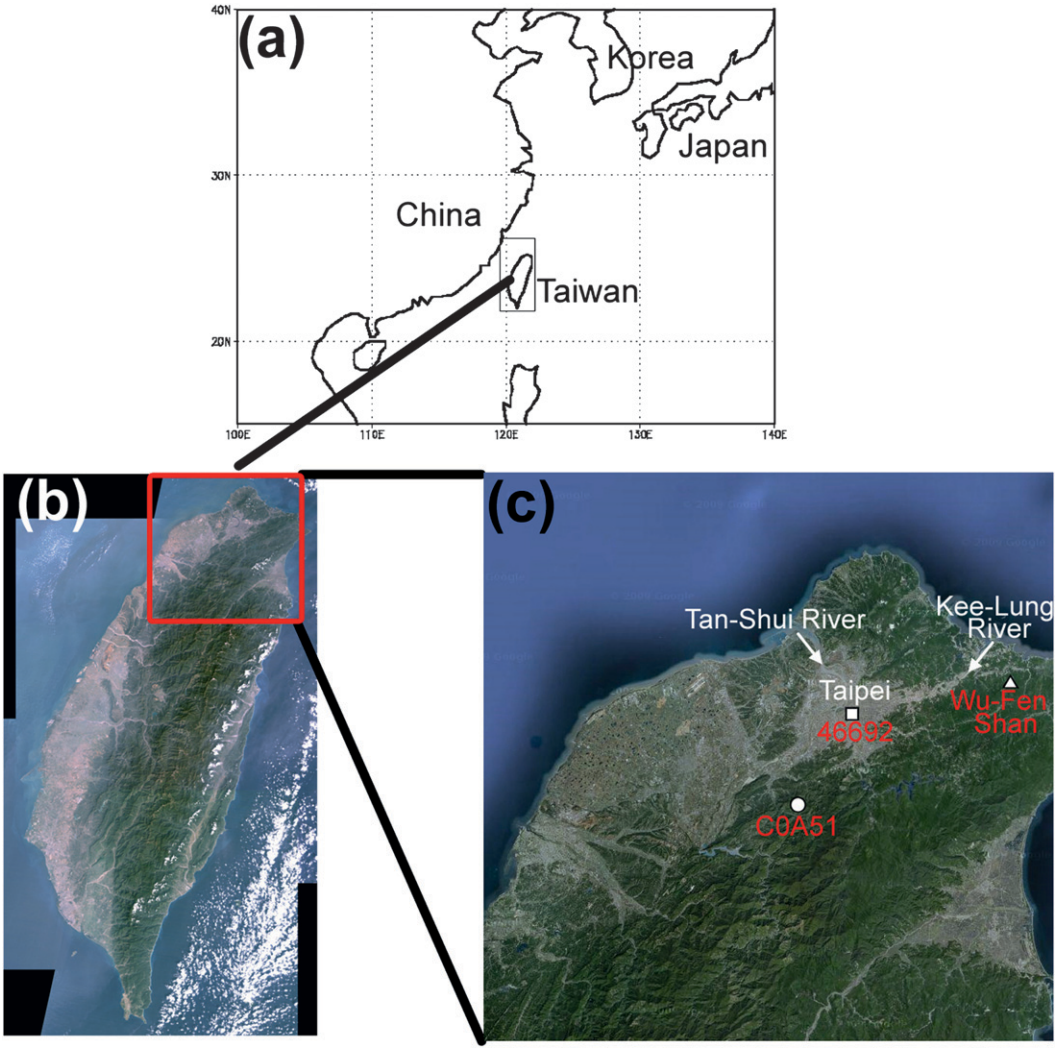

FIG. 1. (a) Location of Taiwan and the surrounding countries. (b) *Landsat 5* satellite image of Taiwan in 1996. (c) Detailed image of northern Taiwan from Google (copyright Google, Inc.) map and the locations of meteorological stations 46692 and C0A51 and Wu-Fen Shan radar station.

b. Model configuration

In this study, the Yonsei University (YSU) (Hong and Dudhia 2003) planetary boundary layer scheme was adopted. The YSU scheme is a modification of the medium-range forecast (MRF) scheme to include explicit entrainment fluxes of heat, moisture and momentum, countergradient transport of momentum, and different specifications of the boundary layer height (BLH).

According to our modeling study (Lin et al. 2008b) the anthropogenic heat (AH) is about 200 W m^{-2} in the urban area. The AH estimation in the Taipei basin is based on energy consumption and population density ratio (Lin et al. 2008b). The source of total energy consumption (including electricity, fuel oil, natural gas, and coal) was obtained from the Bureau of Energy, Ministry of Economic Affairs, Taiwan, in 2005. A detailed description is found in Lin et al. (2008b). The initial and boundary conditions for WRF were obtained from National Centers for Environmental Prediction (NCEP) FNL datasets at 6-h intervals. Four nest domains were constructed with spatial grid resolutions of 27, 9, 3, and 1 km, which contained 150×122, 100×88, 100×160, and 91×79 grid boxes, respectively, from north to south and east to west. In the following discussion, we only show the finest domain (1-km resolution) to compare with the observation. For the urban type in the UCM model, high-intensity residence was employed to represent the high population density in the Taipei area. In this study, we set the model run from

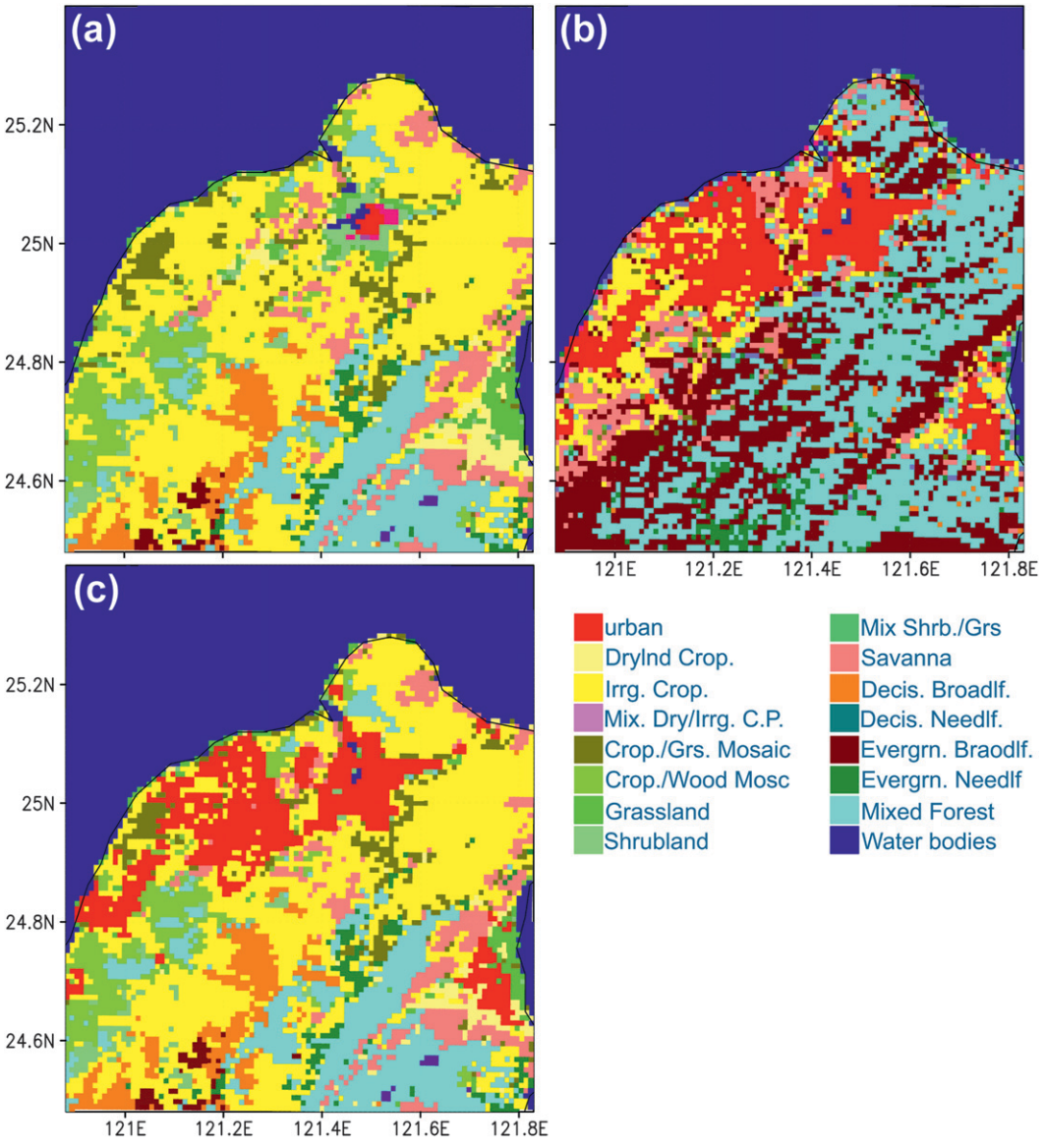

FIG. 2. (a) Original land use in the finest domain of the model provided by USGS. (b) MODIS land use of the finest domain in 2005. (c) Land use as in case USGS but with the urban area replaced with the MODIS dataset. The different colors represent the classification of land use in the USGS and MODIS cases.

1200 UTC (2000 LST) 16 July 2006 and for a total of 36 h for each experiment.

c. *Land use distribution in Taiwan*

Because land use of the original U.S. Geological Survey (USGS) dataset in the model over Taiwan is totally outdated (Lin et al. 2008b), we replaced the original USGS 25-category data over Taiwan with MODIS satellite LU 1-km-resolution data. The MODIS land-cover database, a 1-km product provided on a quarterly basis by the Earth Observing System (EOS)-A platform (*Terra*), is for July 1999. Figures 2a and 2b show the land use classification in the finest domain for the MODIS and USGS cases, respectively. In this study, the impact of land use types and their associated UHI effect on precipitation were examined in the WRF-Noah-UCM model.

3. Observations

a. *Synoptic weather conditions*

To study this issue, a stable weather condition case, namely a Pacific high pressure system dominating the

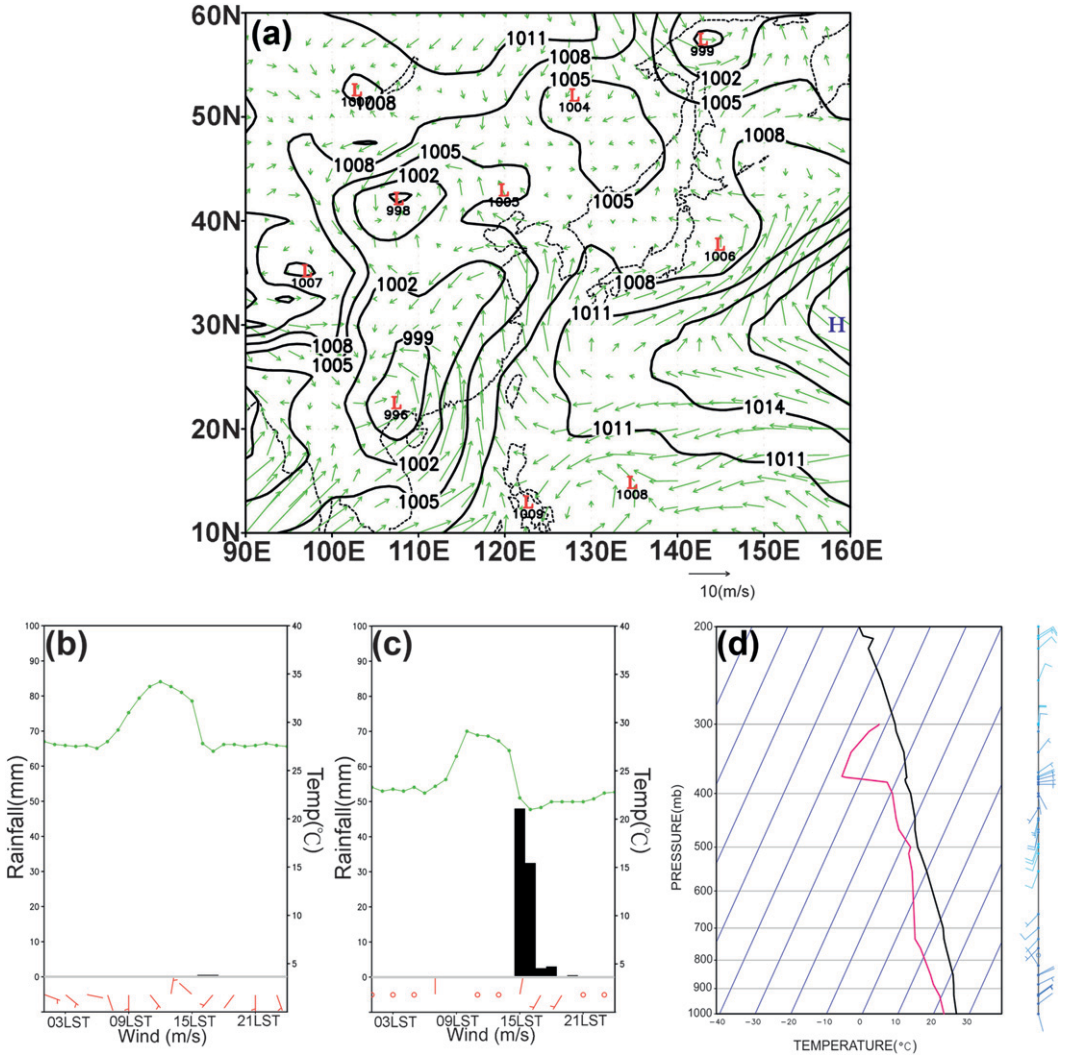

FIG. 3. (a) Surface level pressure and wind field deduced from NCEP data for the study case on 17 Jul 2006. Solid lines represent the surface pressure. The scale of the surface wind vector is shown at the bottom right corner; of the H and L respectively show the location of major high and low pressure systems. (b) Hourly variation of surface air temperature (green), wind field (red), and rainfall (black bar) at urban station 46692. (c) As in (b), but at mountain station C0A51. (d) Morning sounding launched at station 46692 at 0000 UTC 17 Jul 2006. Black line represents air temperature and red is dewpoint temperature.

weather patterns, was used to examine the urbanization effect and its possible impact. Figure 3a, the surface weather map deduced from NCEP data, shows that a high pressure system dominated the weather conditions and that southeasterly winds prevailed on 17 July 2006. The observation of air temperature in Taipei urban station 46692 (25.04°N, 121.51°E, elevation 5.5 m; Fig. 1c) shows that the air temperature ranged from 34° to 35°C around noon and from 27° to 28°C during the nighttime (Fig. 3b). The prevailing wind direction was mainly from the south (Fig. 3b). At the mountain station C0A51 (24.89°N, 121.41°E, elevation 590 m; Fig. 1), the daytime air temperature peaked at about 30°C and dramatically decreased to nearly 20°C when rainfall occurred (Fig. 3c). Figure 3d shows the sounding launched at 0000 UTC (0800 LST) 17 July in northern Taiwan at station 46692. According to calculations from the sounding, the convective inhibition (CIN) was nearly 81.6 $m^2 s^{-2}$ and convective available potential energy (CAPE) was as high as 929 $m^2 s^{-2}$. The level of free convection (LFC) was around 758 hPa (2471 m). The convection K-index was 32.5 and the total index was 46.2. The conditions were favorable for convection development once the air masses were lifted to the LFC. Actually, this was a typical summer thunderstorm case with a high surface air temperature during daytime,

accompanied by a definite land sea breeze over northern Taiwan.

b. Rainfall patterns, wind field, and radar data

Figure 4 shows the horizontal distribution of observation wind field and rainfall amount at the Central Weather Bureau monitoring stations in northern Taiwan. It is clear that a sea breeze developed along the Tan-Shui and Kee-Lung rivers and combined with the upslope flow to reach the mountainous area around noon (Fig. 4a). Precipitation first occurred downwind of the Taipei metropolis over the mountainous area at 1400 LST (Fig. 4b). This was identified by the radar reflectivity observed by the CWB Wu-Fen Shan radar station (Fig. 1). In other words, at 1400 LST the first intensity radar echo was observed over the mountainous area downwind of Taipei (Fig. 5a). Radar reflectivity echo and rainfall record both indicated that the rainfall system was well organized and enhanced between 1500 and 1600 LST (Figs. 4c,d and 5b,c). After 1600 LST the enhanced rainfall was located to the south and west of Taipei (Figs. 4d and 5c,d). Concurrently, the wind direction over the city significantly changed from a northwesterly (sea breeze) into a southwesterly because of the downdraft of the rainfall system over the lower slope and plain area after 1600 LST (Fig. 4d). Accumulated daily rainfall (Fig. 4e) and the intensity of radar reflectivity (Figs. 5b–d) in this episode displayed a nearly north–south direction along 121.4°E.

4 Simulation results and discussion

a. Distribution of accumulation rainfall

Figures 6a and 6b show the accumulation of rainfall amount for the model simulation with different land use classifications for the MODIS satellite (the MODIS case) and original USGS data (the USGS case), respectively, on 17 July 2006. Over the mountainous area, a clear accumulation rainfall amount greater than 50 mm was distributed at around 121.4°E in a north–south direction from the mountain slope to the plain area in the MODIS case. Our simulation results simulated this accumulation precipitation pattern very well when comparing the rainfall record (Fig. 4e). In contrast, there was no significant intense rainfall pattern over the lower slope and plain areas in the USGS case (Fig. 6b). However, there are relatively large areas where crop land has been changed into forest in MODIS as compared to USGS (Figs. 2a,b). To identify the roles played by the change of crop land to forest over the mountain areas, a sensitivity study (called USGS-urban) was conducted with land use being kept the same as in the USGS case, except for the urban area that was replaced with the MODIS dataset (Fig. 2c). Figure 6c shows the spatial distribution of the accumulation rainfall in USGS-urban. The accumulation rainfall still maintained a north–south distribution similar to the MODIS case. It is important to note that the correct use of the urban area played a key role in the performance of the simulated rainfall distribution. In other words, the UHI effect could have significantly disturbed the thermal and dynamical processes for the formation of a rainfall system and hence impacted the location of the rainfall. Moreover, as described in our previous study (Lin et al. 2008b), anthropogenic heating plays an important role in boundary layer development. The question arose as to whether this effect could also impact the precipitation. With this in mind, we further examined the role of anthropogenic heating in the MODIS case. Figure 6d shows the sensitivity study (called the NOAH case), which had the same model configurations as in MODIS, except for anthropogenic heating being turned off. Figure 6d shows that the simulation result also failed to present accumulation rainfall over the lower slope and plain areas. The enhanced thermal effect joined by AH is also crucial to the distribution of rainfall in northern Taiwan.

b. Rainfall formation processes

Following the above modeling results, the scientific questions are how and why land use changes and the associated UHI effect could have such a significant impact on those processes. In further examining the discrepancies between observations and simulation results, we found rainfall northward over the low slope and plain areas between 1600 and 1700 LST for the MODIS case (Figs. 7a–d). However, significant precipitation mainly occurred around 1400–1500 LST over the mountainous areas and decreased quite soon after 1500 LST for the USGS case (Figs. 8a–d). Actually, no significant rainfall occurred after 1600 LST over the mountain and plain area for USGS (Figs. 8a–d). Moreover, the enhanced observation rainfall and radar reflectivity over northern Taiwan distributed in a north–south direction occurred between 1500 and 1600 LST (Figs. 4 and 5), and they weakened significantly after 1800 LST. Although the enhanced precipitation in MODIS occurred 1–2 h later than in USGS, the performance of the simulation distribution for the occurrence of enhanced precipitation in MODIS predicted reasonably better than that in USGS.

To explore the mechanism discrepancy we further examined the differences for thermal and dynamic processes between the USGS and MODIS cases. Figures 9a and 9b show the differences in air temperature (2 m in elevation) and water vapor (the lowest level of the model) between MODIS and USGS. Clearly, the air

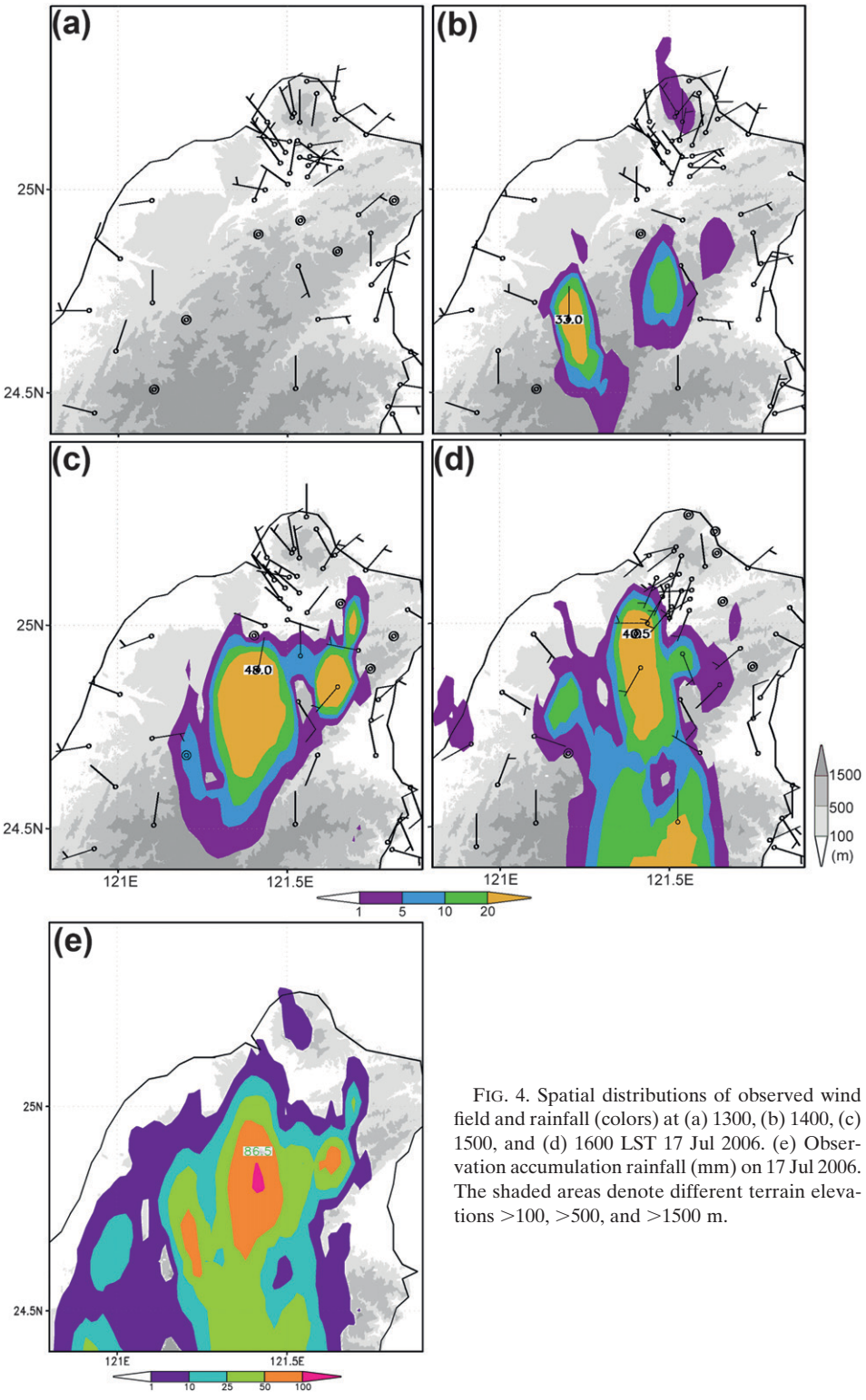

FIG. 4. Spatial distributions of observed wind field and rainfall (colors) at (a) 1300, (b) 1400, (c) 1500, and (d) 1600 LST 17 Jul 2006. (e) Observation accumulation rainfall (mm) on 17 Jul 2006. The shaded areas denote different terrain elevations >100, >500, and >1500 m.

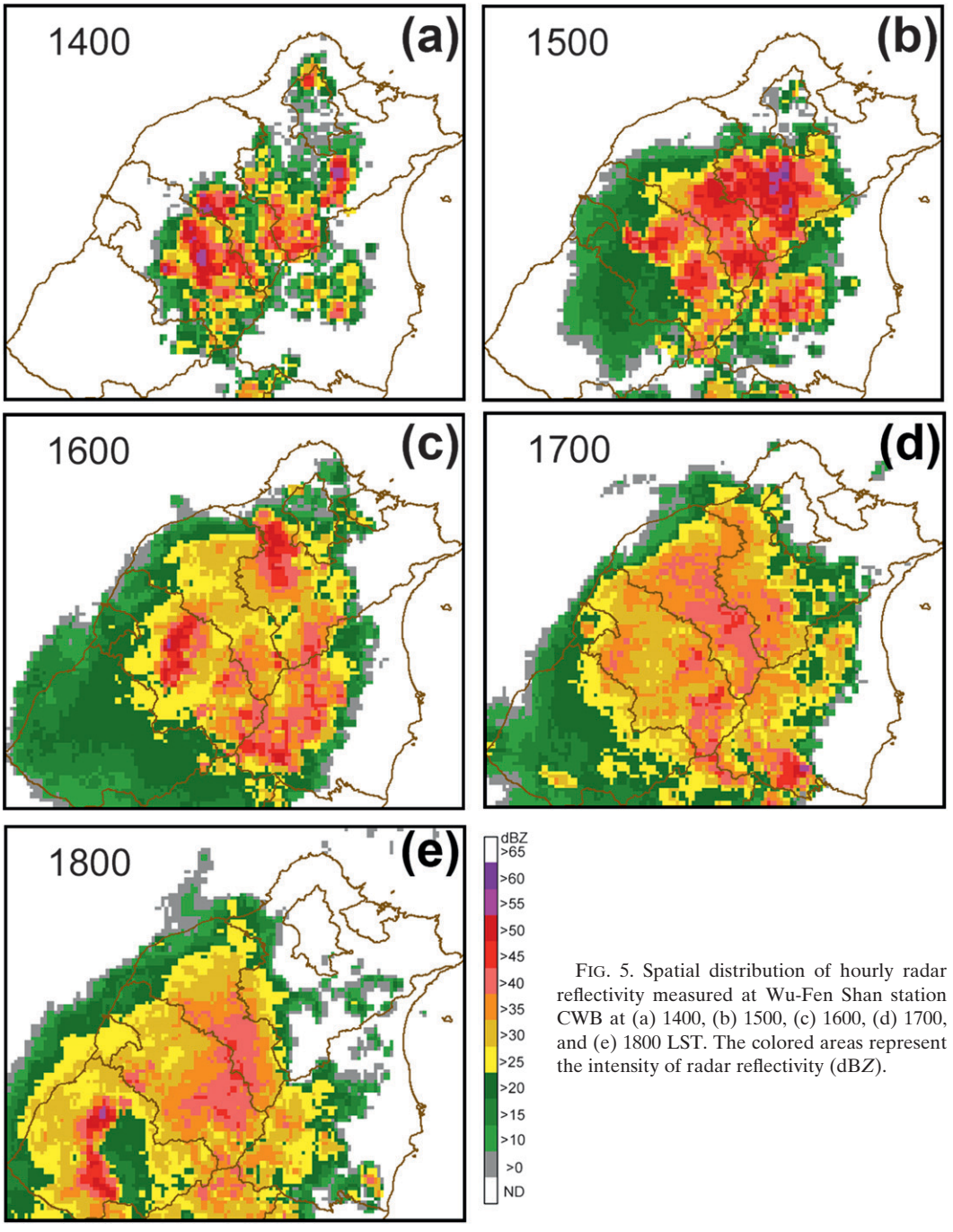

FIG. 5. Spatial distribution of hourly radar reflectivity measured at Wu-Fen Shan station CWB at (a) 1400, (b) 1500, (c) 1600, (d) 1700, and (e) 1800 LST. The colored areas represent the intensity of radar reflectivity (dBZ).

temperature (water vapor) for MODIS was about 2 K (2 g kg^{-1}) higher (less) than that for USGS over the city because of the warm, dry urban center at 1000 LST (Figs. 9a,b). Cities create dry and warm centers with significant evaporation, which is adverse to precipitation formation. In other words, urbanization plays a role in inhibiting water vapor from being transported by sea breeze from the ocean to the inland mountainous area for the MODIS case. Figure 10 shows the horizontal distribution of water vapor flux (near-surface wind speed multiplied by specific humidity) and wind field variation before the rainfall occurred on 17 July 2006 for the MODIS and USGS cases. The magnitude of the water vapor flux is denoted by a color scale; wind speed is represented by arrow. The scale of the near-surface wind vector is shown at the bottom right corner of Fig. 10.

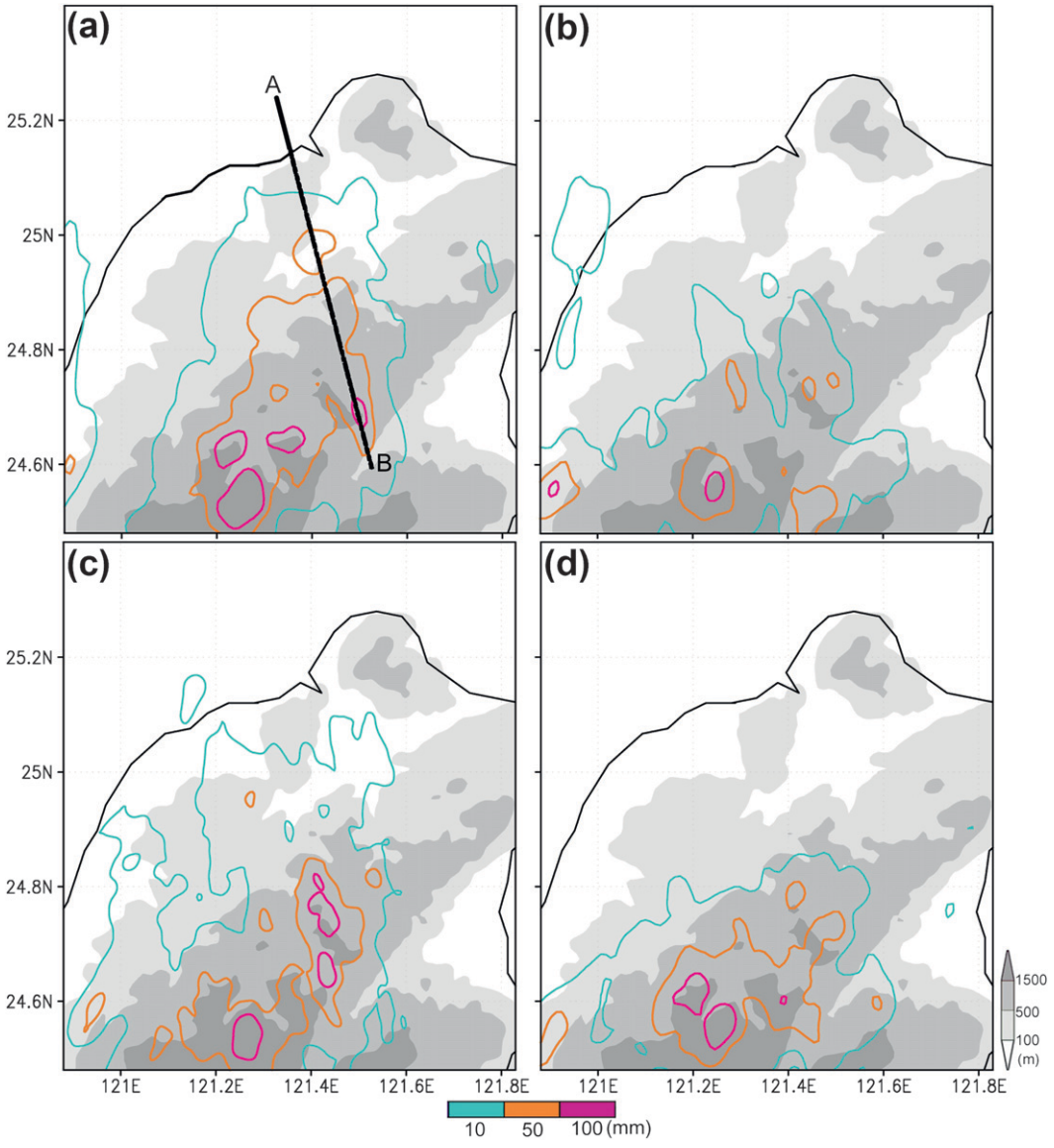

FIG. 6. Simulated accumulation of rainfall for the (a) MODIS, (b) USGS, (c) USGS-urban (same as USGS but the urban area is replaced with MODIS), and (d) NOAH cases (same as MODIS but anthropogenic heating is turned off). The colored contour lines represent rainfall amounts of 10 (blue), 50 (orange), and 100 mm (pink). The shaded areas denote different terrain elevations >100, >500, and >1500 m. Line AB in (a) displays the location of the northwest–southeast cross section in Fig. 11.

In the morning at 1000 and 1100 LST, the moisture flux was less than 50 g kg^{-1} m s^{-1} over the city center and its downwind mountain areas for MODIS (Figs. 10a,c), while the moisture flux was almost as high as 80–100 g kg^{-1} m s^{-1} for USGS at the same time and location (Figs. 10b,d). It is important to note that water vapor in USGS (Figs. 10b,d) could be easily transported to more inland mountainous areas than in MODIS (Figs. 10a,c). This is because USGS has more homogenous land use–cover (mostly dry land or irregular crop) (Fig. 2) and higher latent heat flux. The moisture flux around the high mountainous area (24.7°N, 121.3°E) was much more than 100 g kg^{-1} m s^{-1} at noontime for USGS (Fig. 10f); this was also significantly higher than that of MODIS (around 50 g kg^{-1} m s^{-1}) (Fig. 10e). Apparently, parts of the incoming moist air masses carried by the sea breeze before noontime were counteracted by the drying effect of the city in the MODIS case. Therefore, it might have taken much longer to transport enough moist air masses to the inland mountainous areas in MODIS than in USGS. In other words, precipitation could form earlier in the USGS case as the air

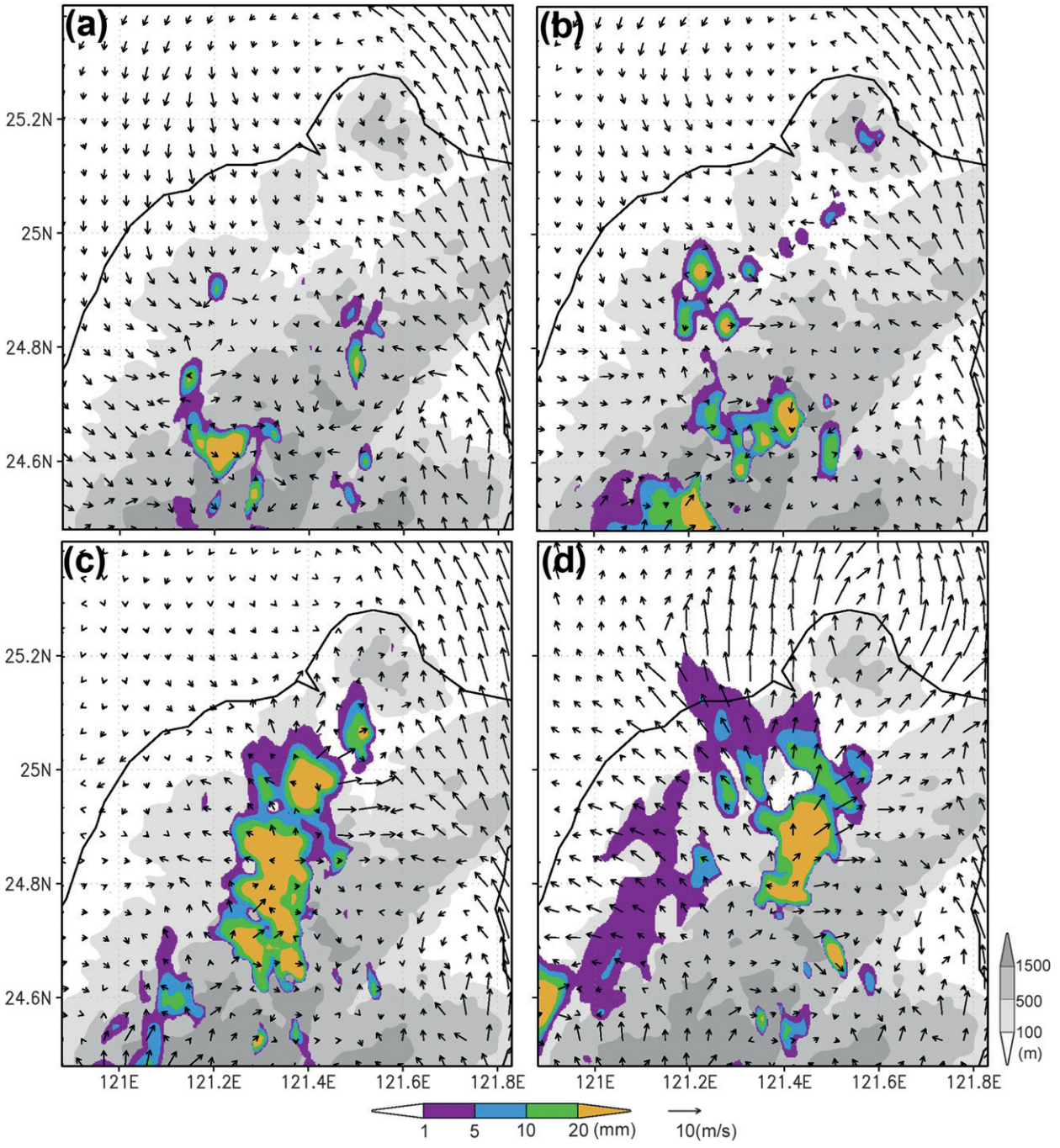

FIG. 7. Simulation hourly rainfall for the MODIS case at (a) 1500, (b) 1600, (c) 1700, and (d) 1800 LST. The colored areas represent rainfall amounts >1, >5, >10, and >20 mm. The shaded areas denote different terrain elevations >100, 500, and 1500 m.

masses with abundant moisture were lifted by the mountain to reach the level of LFC earlier than in the MODIS case. This is the reason why the rainfall system could develop and dump rainfall rapidly in USGS whereas precipitation developed about 2 h later in MODIS. On the other hand, the atmospheric conditions turned more unstable in the MODIS case owing to enhanced sensible heating by the urban area and its roughness (Lin et al. 2008b), which facilitated the upward motion to reach LFC, thus resulting in the significant rainfall later on. Compared to observations, the MODIS case simulated reasonably well because of its correct and detailed land use classification and resulting thermal and dynamic processes.

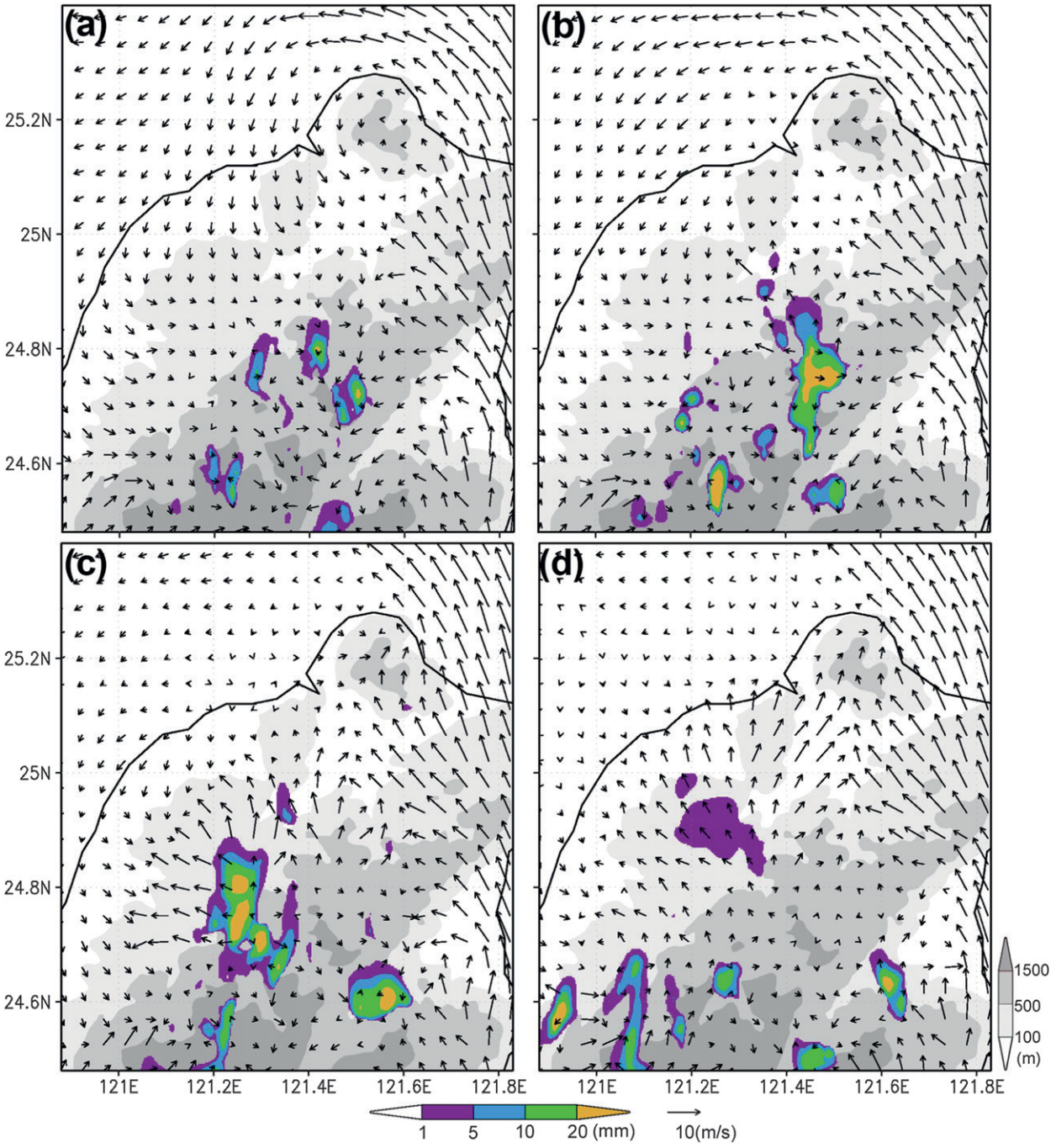

FIG. 8. As in Fig. 7, but for the USGS case: (a) 1300, (b) 1400, (c) 1500, and (d) 1600 LST.

Figure 11 provides another way to examine the dynamic and thermal processes associated with the rainfall system development derived from cross section AB in Fig. 6a. The color shades represent the water vapor mixing ratio. The well-mixed air masses (air masses with 306 K) could reach as high as 850 hPa (around 1.5 km) over the city because of the high sensible heat flux and significant upward motion along this cross section (Fig. 11a). In contrast, air masses with 306 K were below 900 hPa for the USGS case (Fig. 11b) and no significant upward motion was found at the same location. At 1400 LST, enhanced rainfall occurred over the high mountainous area for USGS (Fig. 11d) while only light rainfall occurred in MODIS (Fig. 11c). Figure 11e shows that

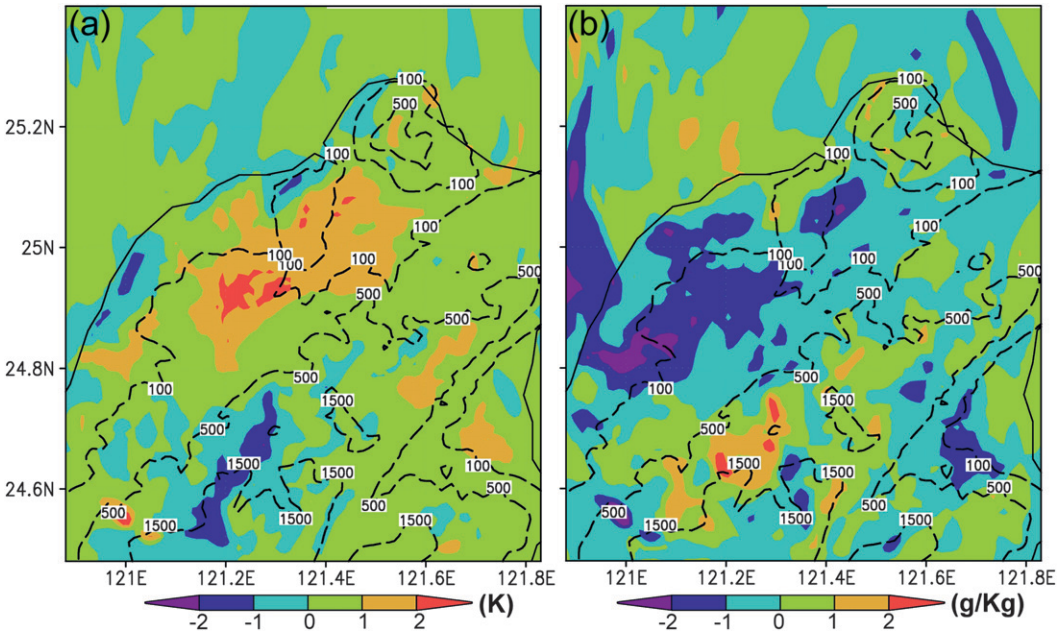

FIG. 9. Differences between the MODIS and USGS cases (MODIS − USGS) at 1000 LST for (a) 2-m air temperature and (b) water vapor mixing ratio at 1000 hPa. The scales of the differences of 2-m air temperature and water vapor mixing ratio are denoted by color shades. The dashed lines denote different terrain elevations.

a significant rainfall system occurred at around 121.41°E along the cross section over the plain for MODIS, resulting in an interaction between the rainfall system over the mountain and persistent incoming moisture carried by the sea breeze after 1600 LST (Figs. 11e,g). However, there was no precipitation for USGS along this cross section after 1600 LST (Figs. 11f,h). Again, the simulation results suggest that urbanization could significantly disturb the thermal and dynamic processes of the precipitation system and hence affect the location of the rainfall system. This is a particularly important implication for water resource management in Taiwan given its complex geographic environment and high population density.

5. Summary

In this study, a next-generation mesoscale model WRF coupled with the Noah land surface model and an urban canopy model was employed to study the UHI impact on precipitation over the complex geographic environment of northern Taiwan. Data show that a significant Pacific high dominated the weather pattern around Taiwan and that a southerly wind prevailed during the study period. The surface air temperature could reach as high as nearly 35°C, and this is attributed to the high sensible heat flux around noon on 17 July 2006. Radar reflectivity indicated that significant echo first occurred at around 1400 LST over the downwind area of the city at high mountainous areas. Then, the rainfall system was enhanced between 1400 and 1600 LST, and after 1600 LST it moved down to the plain area surrounding the urban area.

Simulation results suggest that urbanization acted as a warm and dry center and hence prevented water vapor from being transported by the sea breeze to the mountainous area. Simulation results also indicated that those adverse factors can delay thunderstorm development. On the other hand, the air mass turned more unstable over and downwind of the city in the MODIS case than in the USGS case because of the enhanced sensible heat flux. Comparing radar reflectivity and rainfall data, our modeling results simulated reasonably well for the timing of the rainfall system formation and its locations. The correct land use classification is crucial for the modeling study because it helps to develop reasonable thermal and dynamic processes and hence leads to reasonably better simulations. Sensitivity testing indicated that anthropogenic heat also plays an important role in the impact on precipitation formation over northern Taiwan.

Our results identify the different features of the precipitation locations over the downwind area of the city. The results also show that urbanization could affect precipitation over upstream plain areas. This situation is quite different from other places with urban areas located over large plain areas resulting in increased rainfall downwind of the city (Steiger et al. 2002; Shepherd

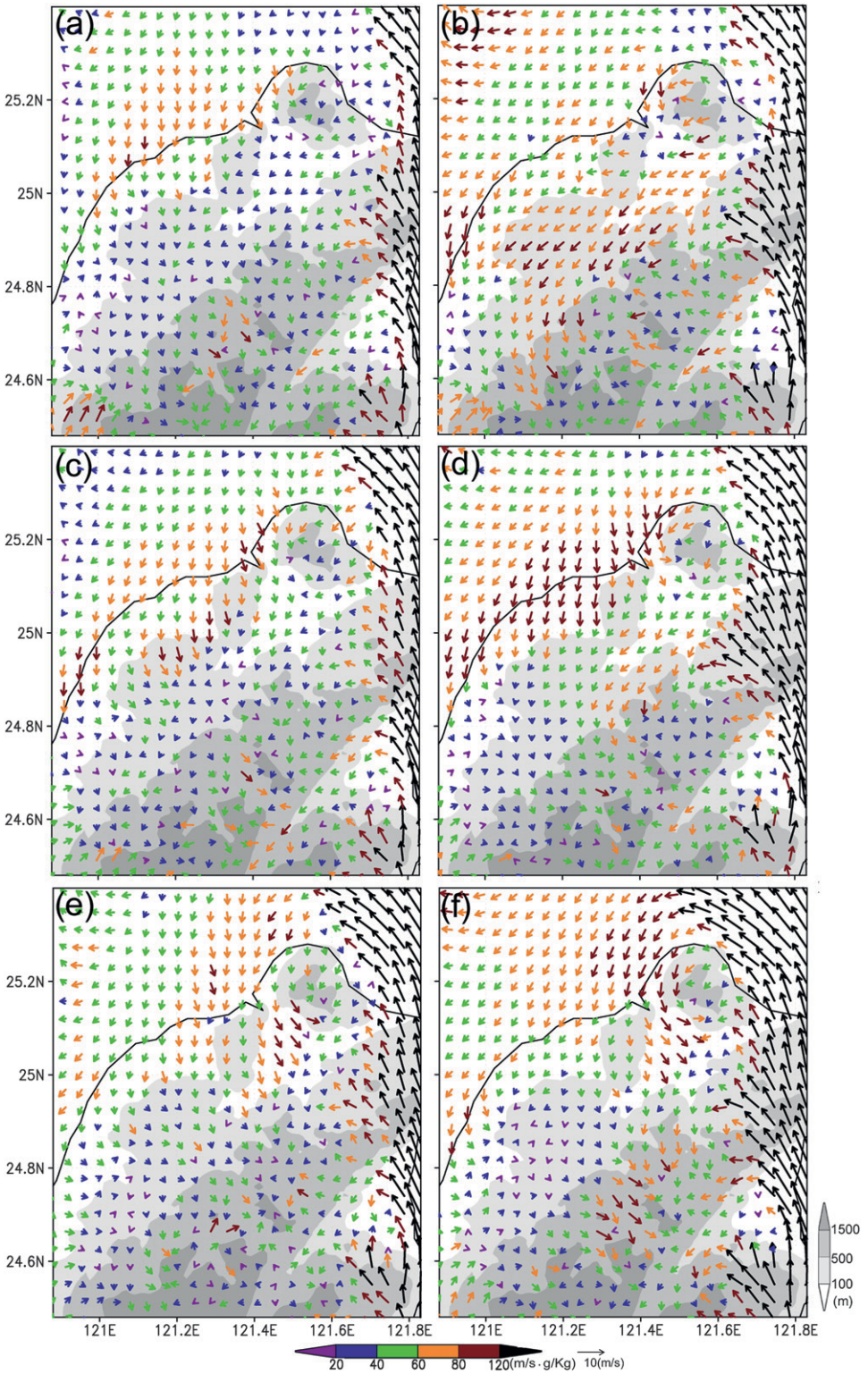

FIG. 10. Spatial distribution of the moisture flux for the MODIS and USGS cases. The scale of the water vapor flux is denoted by colors. Surface wind speed is represented by arrows. The scale of the surface wind vector is shown at the bottom right corner. Cases shown are (a) MODIS at 1000 LST, (b) USGS at 1000 LST, (c) MODIS at 1100 LST, (d) USGS at 1100 LST, (e) MODIS at 1200 LST, and (f) USGS at 1200 LST.

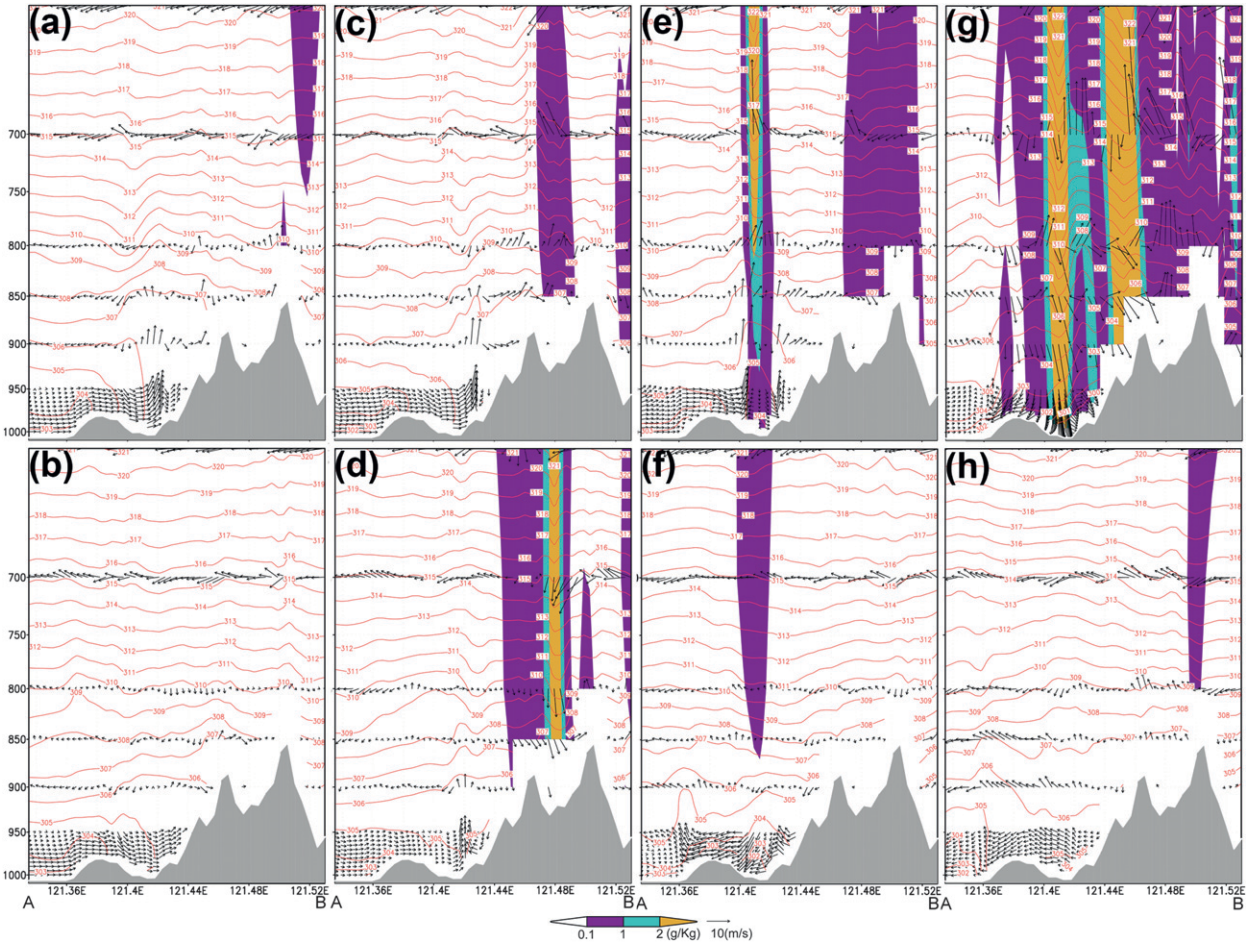

FIG. 11. Vertical distributions of the potential temperature (contour), wind field, and water vapor mixing ratio (g kg^{-1}) (color shades) along cross-sectional line AB in Fig. 6a. Cases shown are (a) MODIS at 1200 LST, (b) USGS at 1200 LST, (c) MODIS at 1400 LST, (d) USGS at 1400 LST, (e) MODIS at 1600 LST, (f) USGS at 1600 LST, (g) MODIS at 1700 LST, and (h) USGS at 1700 LST.

et al. 2002). This study provides important data for water resource management and future city planning over northern Taiwan with its complex geographic environment and high population density.

Acknowledgments. This work was supported by grants from Academia Sinica Taiwan under the theme project "Heat island effect over Taiwan's western plain and its impacts on climate changes" (AS-93-TP-A04) and by NSC 96-2111-M-001-004-MY3.

REFERENCES

Arnfield, A. J., 2003: Two decades of urban climate research: A review of turbulence, exchanges of energy and water, and the urban heat island. *Int. J. Climatol.,* **23,** 1–26.

Atkinson, B. W., 2003: Numerical modeling of urban heat island intensity. *Bound.-Layer Meteor.,* **109,** 285–310.

Baik, J.-J., Y.-H. Kim, and H.-Y. Chun, 2001: Dry and moist convection forced by an urban heat island. *J. Appl. Meteor.,* **40,** 1462–1475.

Balling, R. C., and R. S. Cerveny, 1987: Long-term associations between wind speeds and the urban heat island of Phoenix, Arizona. *J. Climate Appl. Meteor.,* **26,** 712–716.

Bornstein, R. D., 1968: Observation of the urban heat island effect in New York city. *J. Appl. Meteor.,* **7,** 575–582.

——, and Q. Lin, 2000: Urban heat islands and summertime convective thunderstorms in Atlanta: Three case studies. *Atmos. Environ.,* **34,** 507–516.

Chen, C.-S., W.-C. Chen, and W.-K. Tao, 2004: Characteristics of heavy summer rainfall in southwestern Taiwan in relation to orographic effects. *J. Meteor. Soc. Japan,* **82,** 1521–1543.

——, ——, Y.-L. Chen, P.-L. Lin, and H.-C. Lai, 2005: Investigation of orographic effects on two heavy rainfall events over southwestern Taiwan during the mei-yu season. *Atmos. Res.,* **73,** 101–130.

Chen, F., and J. Dudhia, 2001: Coupling an advanced land surface–hydrology model with the Penn State–NCAR MM5 modeling system. Part I: Model implementation and sensitivity. *Mon. Wea. Rev.,* **129,** 569–585.

——, H. Kusaka, M. Tewari, J.-W. Bao, and H. Kirakuchi, 2004: Utilizing the coupled WRF/LSM/Urban modeling system with detailed urban classification to simulate the urban heat island phenomena over the greater Houston area. *Extended Abstracts,*

Fifth Conf. on Urban Environment, Vancouver, BC, Canada, Amer. Meteor. Soc., 9.11. [Available online at http://ams.confex.com/ams/pdfpapers/79765.pdf.]

Chen, T.-C., S.-Y. Wang, and M.-C. Yen, 2007: Enhancement of afternoon thunderstorm activity by urbanization in a valley: Taipei. *J. Appl. Meteor. Climatol.,* **46,** 1324–1340.

Corburn, J., 2009: Cities, climate change, and urban heat island mitigation: Localizing global environmental science. *Urban Stud.,* **46,** 413–427.

Dixon, P. G., and T. L. Mote, 2003: Patterns and causes of Atlanta's urban heat island–initiated precipitation. *J. Appl. Meteor.,* **42,** 1273–1284.

Ek, M. B., K. E. Mitchell, Y. Lin, E. Rogers, P. Grunmann, V. Koren, G. Gayno, and J. D. Tarpley, 2003: Implementation of Noah land surface model advances in the National Centers for Environmental Prediction operational mesoscale Eta model. *J. Geophys. Res.,* **108,** 8851, doi:10.1029/2002JD003296.

Feddema, J. J., K. W. Oleson, G. B. Bonan, L. O. Mearns, L. E. Buja, G. A. Meehl, and W. M. Washington, 2005: The importance of land-cover change in simulating future climates. *Science,* **310,** 1674–1678.

Grimmond, C. S. B., and T. R. Oke, 1995: Comparison of heat fluxes from summertime observations in the suburbs of four North American cities. *J. Appl. Meteor.,* **34,** 873–889.

Hjemfelt, M. R., 1982: Numerical simulation of the effects of St. Louis on mesoscale boundary-layer airflow and vertical motion: Simulations of urban vs. non-urban effects. *J. Appl. Meteor.,* **21,** 1239–1257.

Holt, T. R., and J. Pullen, 2007: Urban canopy modeling of the New York City metropolitan area: A comparison and validation of single- and multilayer parameterization. *Mon. Wea. Rev.,* **135,** 1906–1930.

Hong, S.-Y., and J. Dudhia, 2003: Testing of a new non-local boundary layer vertical diffusion scheme in numerical weather prediction applications. *Extended Abstracts, 16th Conf. on Numerical Weather Prediction,* Seattle, WA, Amer. Meteor. Soc., 17.3. [Available online at http://ams.confex.com/ams/pdfpapers/72744.pdf.]

Jin, M., J. M. Shepherd, and M. D. King, 2005: Urban aerosols and their interaction with clouds and rainfall: A case study for New York and Houston. *J. Geophys. Res.,* **110,** D10S20, doi:10.1029/2004JD005081.

Kusaka, H., and F. Kimura, 2004: Coupling a single-layer urban canopy model with a simple atmospheric model: Impact on urban heat island simulation for an idealized case. *J. Meteor. Soc. Japan,* **82,** 67–80.

——, K. Kondo, Y. Kikegawa, and F. Kimura, 2001: A simple single-layer urban canopy model for atmospheric models: Comparison with multi-layer and slab models. *Bound.-Layer Meteor.,* **101,** 329–358.

——, F. Chen, and M. Tewari, 2006: Impact of using the urban canopy model on the simulation of the heat island of Tokyo. *Extended Abstracts, Sixth Symp. on the Urban Environment,* Atlanta, GA, Amer. Meteor. Soc., J1.3. [Available online at http://ams.confex.com/ams/Annual2006/techprogram/paper_104243.htm.]

Lacke, M. C., T. L. Mote, and J. M. Shepherd, 2009: Aerosols and associated precipitation patterns in Atlanta. *Atmos. Environ.,* **43,** 4359–4373.

Lin, C.-Y., and C.-S. Chen, 2002: A study of orographic effects on mountain-generated precipitation systems under weak synoptic forcing. *Meteor. Atmos. Phys.,* **81,** 1–25.

——, W.-C. Chen, S. C. Liu, Y. A. Liou, G. R. Liu, and T.-H. Lin, 2008a: Numerical study of the impact of urbanization on the precipitation over Taiwan. *Atmos. Environ.,* **42,** 2934–2947.

——, F. Chen, J. C. Huang, W.-C. Chen, Y. A. Liou, W. N. Chen, and S. C. Liu, 2008b: Urban heat island effect and its impact on boundary layer development and land–sea circulation over northern Taiwan. *Atmos. Environ.,* **42,** 5639–5649.

Lo, C. P., D. A. Quattrochi, and J. C. Luvall, 1997: Application of high-resolution thermal infrared remote sensing and GIS to assess the urban heat island effect. *Int. J. Remote Sens.,* **18,** 287–304.

Morris, C. J. G., I. Simmonds, and N. Plummer, 2001: Quantification of the influences of wind and cloud on the nocturnal urban heat island of a large city. *J. Appl. Meteor.,* **40,** 169–182.

Mote, T. L., M. C. Lacke, and J. M. Shepherd, 2007: Radar signatures of the urban effect on precipitation distribution: A case study for Atlanta, Georgia. *Geophys. Res. Lett.,* **34,** L20710, doi:10.1029/2007GL031903.

Naccarato, K. P., O. Pinto Jr., and I. R. C. A. Pinto, 2003: Evidence of thermal and aerosol effects on the cloud-to-ground lightning density and polarity over large urban areas of Southeastern Brazil. *Geophys. Res. Lett.,* **30,** 1674, doi:10.1029/2003GL017496.

Oke, T. R., 1982: The energetic basis of the urban heat island. *Quart. J. Roy. Meteor. Soc.,* **108,** 1–24.

Pielke, R. A., J. Adegoke, A. Beltrán-Przekurat, C. A. Hiemstra, J. Lin, U. S. Nair, D. Niyogi, and T. E. Nobis, 2007: An overview of regional land-use and land-cover impacts on rainfall. *Tellus,* **59B,** 587–601.

Ren, G. Y., Z. Y. Chu, Z. H. Chen, and Y. Y. Ren, 2007: Implications of temporal change in urban heat island intensity observed at Beijing and Wuhan stations. *Geophys. Res. Lett.,* **34,** L05711, doi:10.1029/2006GL027927.

Rozoff, C. M., W. R. Cotton, and J. O. Adegoke, 2003: Simulation of St. Louis, Missouri, land use impact on thunderstorms. *J. Appl. Meteor.,* **42,** 716–738.

Shem, W., and M. Shepherd, 2009: On the impact of urbanization on summertime thunderstorms in Atlanta: Two numerical model case studies. *Atmos. Res.,* **92,** 172–189.

Shepherd, J. M., 2005: A review of current investigations of urban-induced rainfall and recommendations for the future. *Earth Interact.,* **9.** [Available online at http://EarthInteractions.org.]

——, H. Pierce, and A. J. Negri, 2002: Rainfall modification by major urban areas: Observation from spaceborne rain radar on the TRMM satellite. *J. Appl. Meteor.,* **41,** 689–701.

Skamarock, W. C., J. B. Klemp, J. Dudhia, D. O. Gill, D. M. Barker, W. Wang, and J. G. Powers, 2005: A description of the Advanced Research WRF version 2, NCAR Tech. Note. NCAR/TN-468+STR, 88 pp.

Steiger, S. M., R. E. Orville, and G. Huffines, 2002: Cloud-to-ground lightning characteristics over Houston, Texas: 1989–2000. *J. Geophys. Res.,* **107,** 4117, doi:10.1029/2001JD001142.

Tewari, M., F. Chen, and H. Kusaka, 2006: Implementation and evaluation of a single-layer urban canopy model in WRF/Noah. *Proc. Seventh WRF Users' Workshop,* Boulder, CO, NCAR. [Available online at http://www.mmm.ucar.edu/wrf/users/workshops/WS2006/abstracts/Session05/5_6_Tewari.pdf.]

Thielen, J., W. Wobrock, A. Gadian, P. G. Mestayer, and J.-D. Creutin, 2000: The possible influence of urban surfaces on rainfall development: A sensitivity study in 2D in the meso-γ-scale. *Atmos. Res.,* **54,** 15–39.

van den Heever, S. C., and W. R. Cotton, 2007: Urban aerosol impacts on downwind convective storms. *J. Appl. Meteor. Climatol.,* **46,** 828–850.